

Fermi National Accelerator Laboratory

FERMILAB-CONF-90/196-T

September 1990

TOP QUARK MASS SPECTRUM FROM
FLAVOR-CHANGING PROCESSES*

Carl H. ALBRIGHT

Department of Physics, Northern Illinois University, DeKalb, Illinois 60115†

and

Fermi National Accelerator Laboratory, P.O. Box 500, Batavia, Illinois 60510‡

Abstract

The input from flavor-changing processes is reviewed and results of several analyses are presented on the top quark mass spectrum without recourse to the neutral-current data. A top quark mass in the range 135 ± 25 GeV is much preferred, but a very massive top quark above 300 GeV can not be ruled out. Comments are made about the future use of the inclusive decay $B \rightarrow \gamma + X_{S=1}$ for constraining the top quark mass.

*To appear in Proceedings of the 25th International Conference on High Energy Physics, Singapore, 1990

†Permanent address

‡BITNET Address: ALBRIGHT@FNAL



The top quark mass spectrum can be obtained from data on flavor-changing processes, without recourse to neutral-current data. The point is, in the standard model, only the basic weak charged-current interactions are flavor-changing. To the extent that loop diagrams involving these interactions and the top quark dominate a calculation, the size of the effect calculated will be governed by the mass of the top quark. Such situations arise for the x_d mixing parameter in $B - \bar{B}$ mixing, for the CP-violation parameters ϵ and ϵ' in the K system, and for the amplitudes for rare K and B decays. When these quantities are well-determined experimentally, one can try to invert the procedure to determine the acceptable range of top quark masses. This is the case for the first three singled out, and a review of the results obtained for the top quark mass spectrum is presented here for several types of analyses. The inclusive decay $B \rightarrow \gamma + X_{S=1}$ is given as an example of a rare decay process which will play a similar role in determining the top quark mass in the near future.

THREE-FAMILY MIXING MATRIX

We begin with the three-family Cabibbo-Kobayashi-Maskawa (CKM) mixing matrix [1]. With the now standard convention, this matrix assumes the following forms in the small-angle approximation and Wolfenstein parametrization [2]:

$$\begin{aligned}
 V_{CKM} &\simeq \begin{pmatrix} 1 & s_{12} & s_{13}e^{-i\delta} \\ -s_{12} & 1 & s_{23} \\ V_{td} & V_{ts} & 1 \end{pmatrix} \\
 &\simeq \begin{pmatrix} 1 - \frac{\lambda^2}{2} & \lambda & A\lambda^3(\rho - i\eta) \\ -\lambda & 1 - \frac{\lambda^2}{2} & A\lambda^2 \\ A\lambda^3(1 - \rho - i\eta) & -A\lambda^2 & 1 \end{pmatrix}
 \end{aligned} \tag{1}$$

where $s_{12} = \sin \theta_{12}$, etc. and δ is the CP-violating phase. One can adopt the convention where all three mixing angles lie in the first quadrant and the phase is restricted to the interval $0 < \delta < \pi$.

The orthogonality property of the first and third columns leads to the unitarity triangle

$$V_{td} + s_{13}e^{i\delta} \simeq s_{12}s_{23} \quad (2)$$

in the complex plane, where the legs of the triangle are determined by $B - \bar{B}$ mixing and the $b \rightarrow u$ and $b \rightarrow c$ transitions. If one normalizes the length of the real leg to unity so the two vertices are at the origin and (1,0), the third vertex is located at (ρ, η) in the complex plane in terms of these two Wolfenstein parameters. On the other hand, the area of the triangle is related to the Jarlskog J-value [3] which is a measure of CP violation

$$\begin{aligned} J &= \text{Im}(V_{us}V_{cb}V_{ub}^*V_{cs}^*) \\ &\simeq s_{12}s_{23}s_{13} \sin \delta \simeq A^2\lambda^6\eta \\ &\sim O(3 \times 10^{-5}) \end{aligned} \quad (3)$$

The range for V_{cb} is given by $V_{cb} = 0.046 \pm 0.006$ as determined from the $\Gamma(b \rightarrow c)$ decay rate [4], while the V_{ub}/V_{cb} ratio recently determined from the inclusive semileptonic B decay spectrum by the ARGUS and CLEO groups [5] leads to the model-dependent result

$$\left| \frac{V_{ub}}{V_{cb}} \right| \sim \frac{s_{13}}{s_{23}} = 0.10 \pm 0.03 \quad (4)$$

The unitarity triangle thus constrains $|V_{td}|$ to the range $|V_{td}| \simeq 0.0036 \rightarrow 0.0182$.

TOP MASS DEPENDENCE

$\Delta B = 2$ $B_d^0 - \bar{B}_d^0$ Mixing

Turning to the flavor-changing loop diagrams, we note that the t-quark exchange box diagram dominates the calculation [6] for the $B - \bar{B}$ mixing parameter x_d [5]

$$x_d = \frac{\Delta m}{\Gamma} = 0.66 \pm 0.09 \quad (5)$$

$$= \frac{G_F^2 M_W^2}{6\pi^2} m_B \tau_B (B_B f_B^2) |V_{td}^* V_{tb}|^2 \eta_{QCD}(x_t) S(x_t)$$

where $x_t = m_t^2/M_W^2$. Note that it involves the absolute square of the V_{td} element, the B decay constant f_B and bag parameter B_B arising from the hadronic matrix elements, the Inami - Lim [7] box function S and QCD correction factor η_{QCD} . The product $B_B f_B^2$ is poorly determined to be $B_B f_B^2 \sim (120 - 180 \text{ MeV})^2$. An important theoretical result for a very massive top follows from the next-to-leading QCD correction calculation of Buras, Jamin and Weisz [8]. They find that although the product of η and S is invariant to the definition of m_t , only if the box function S is evaluated at the running top mass will the QCD correction factor be nearly independent of m_t , with $\eta_{QCD} \sim 0.84$. The bottom line is that since $\eta_{QCD} S \sim m_t^2 R(m_t)$, where $R(m_t)$ rolls off slowly, smaller values of $B_B f_B^2$ and smaller $|V_{td}|$ favor larger m_t , with the largest m_t occurring with δ in the first quadrant.

$\Delta S = 2$ Indirect CP-Violation Parameter ϵ

The weak eigenstates K_S and K_L are related to the CP eigenstates K_1 and K_2 through the "wrong" CP eigenstate admixture parameter ϵ by

$$K_S = K_1 + \epsilon K_2, \quad K_L = \epsilon K_1 + K_2 \quad (6)$$

where

$$\begin{aligned} \epsilon &= \frac{i\text{Im}M_{12} + i\text{Im}\Gamma_{12}}{(m_L - m_S) - i(\Gamma_L - \Gamma_S)/2} \simeq \frac{\text{Im}M_{12}}{\sqrt{2}\Delta m} e^{i43.7^\circ} \\ &= (2.259 \pm 0.018) \times 10^{-3} e^{i43.7^\circ} \end{aligned} \quad (7)$$

Box diagrams involving both top- and charm-quark exchange contribute to the theoretical determination of ϵ , and one finds [9]

$$\begin{aligned} \text{Im}M_{12} &= \frac{G_F^2 M_W^2}{12\pi^2} m_K (B_K F_K^2) \text{Im} \left[(V_{td}^* V_{ts})^2 \eta_2 S_2 + \dots \right] \\ &\simeq \frac{G_F^2 M_W^2}{6\pi^2} m_K (B_K F_K^2) J [V_{ud}^2 (V_{cb}^2 \end{aligned}$$

$$- \frac{V_{cs}}{V_{us}} |V_{ub}| |V_{cb}| \cos \delta \eta_2(x_t) S_2(x_t) + \dots \quad (8)$$

in terms of the CP-violating parameter J , the QCD correction factor η_2 and the Inami-Lim function S_2 , where we have spelled out just the leading top-exchange contribution for a massive top. The imaginary part of the square of the V_{td} element enters, which involves $\cos \delta$, and helps to unravel the 1st and 2nd quadrant ambiguity for δ . The major uncertainty here involves the bag parameter B_K , which has recently been narrowed to the range 0.55 - 0.90 from calculations of Buras et al. [10] on the leading order corrections to the $1/N$ expansion result. The next-to-leading QCD correction calculation of ref. [8] indicates that $\eta_2(x_t) \sim 0.57$ and nearly a constant, if S_2 is evaluated at the running top mass $\bar{m}_t(m_t)$. Note that smaller B_K and smaller J favor larger m_t , again with the larger m_t occurring with δ in the first quadrant.

$\Delta S = 1$ Direct CP-Violation Parameter ϵ'

The CP parameters ϵ and ϵ' are related to the experimentally-accessible quantities η_{+-} and η_{00} by

$$\begin{aligned} \eta_{+-} &\equiv \frac{A(K_L \rightarrow \pi^+ \pi^-)}{A(K_S \rightarrow \pi^+ \pi^-)} = \epsilon + \epsilon' \\ \eta_{00} &\equiv \frac{A(K_L \rightarrow \pi^0 \pi^0)}{A(K_S \rightarrow \pi^0 \pi^0)} = \epsilon - 2\epsilon' \end{aligned} \quad (9)$$

leading to the Wu-Yang triangle [11] in the complex plane. Since the last conference in '88, we have a second determination of ϵ'/ϵ by the E731 group at Fermilab, but unfortunately the CERN and Fermilab numbers [12] disagree:

$$\epsilon'/\epsilon = \begin{cases} (33 \pm 11) \times 10^{-4} & (NA31) \\ (-4 \pm 15) \times 10^{-4} & (E731) \end{cases} \quad (10)$$

Following the work of ref. [13] in the mid-70's it has been known that for low top masses, the major contribution to ϵ'/ϵ comes from the QCD penguin diagram. In the

notation of Buchella et al. [14],

$$\frac{\epsilon'}{\epsilon} = \frac{G_F r s_{12} J}{\sqrt{2} \text{Re} A_0} y_6 \langle Q_6 \rangle_0 (1 - \bar{\Omega}) \quad (11)$$

where $\bar{\Omega}$ represents additional contributions beyond the simple QCD penguin diagram. At large top masses, the photon penguin and, more importantly, the Z penguin, play important roles. In fact, both ref. [14] and Paschos et al. [15] have shown that the corrections from the electroweak penguins can become so large that they overwhelm the QCD penguin contribution and drive ϵ'/ϵ negative for $m_t > 220$ GeV.

TOP QUARK MASS SPECTRUM

Now we turn to the top quark mass spectrum determined from these flavor-changing processes. The analyses fall into several categories.

Allowed $\rho - \eta$ Region for Fixed m_t

One can plot the allowed regions in the Wolfenstein ρ vs. η parameter space for different m_t after the constraints from the processes of the above Section have been imposed. A recent analysis of this type has been published by Dib, Dunietz, Gilman and Nir [16].

Scatter Plot of m_t vs. $F_B \sqrt{B_B}$

By fixing $F_K \sqrt{B_K}$ for the K system, Gunion and Gradkowski [17] obtain an apparent 2-band structure when they plot m_t vs. $F_B \sqrt{B_B}$. Comparable results [18] are obtained by Buchalla, Buras and Harlander as well as Cocolicchio and Cudell.

Global Fits to All the Mixing Data

Making use of the Wolfenstein parametrization for V_{CKM} , Kim, Rosner and Yuan [19] have performed a least squares fit of all the mixing data and present chi-square contours in the η vs. m_t plane. If no ϵ'/ϵ data is used, they find two probability peaks located at

$$m_t = 122^{+54}_{-37} \text{ GeV} \quad \text{and} \quad m_t = 401^{+398}_{-192} \text{ GeV} \quad (12)$$

They used $B_B F_B^2 = (140 \pm 40 \text{ MeV})^2$. Maalampi and Roos [20] have also attempted a least squares fit and find $m_t = 154 \pm 29 \text{ GeV}$, with an extremely large $B_B F_B^2$ value, however.

Quark Mass Matrix Approach

A brief description of the quark mass matrix approach follows which the author used to obtain the top quark mass spectrum as described in more detail in ref. [21].

Start with a modified set of Fritzsch mass matrices of the form

$$\mathbf{M}^U = \begin{pmatrix} 0 & A & D \\ A & E & B \\ D^* & B & C \end{pmatrix}, \quad \mathbf{M}^D = \begin{pmatrix} 0 & A' & D' \\ A'^* & E' & B' \\ D'^* & B'^* & C' \end{pmatrix} \quad (13a)$$

with the relaxed hierarchy

$$\begin{aligned} |A|, |E|, |D| &\ll |B| \ll C, \\ |A'|, |E'|, |D'| &\ll |B'| \ll C' \end{aligned} \quad (13b)$$

Recall that the skew diagonals vanish in the Fritzsch model [22], and the largest possible top quark mass is approximately 100 GeV, as bounded by the CKM mixing matrix. With squares of the diagonal matrices related by unitary transformations to

the mass matrices of (13a) in the weak basis

$$\begin{aligned} (\mathbf{D}^U)^2 &= U_L(\mathbf{M}^U\mathbf{M}^{U\dagger})U_L^\dagger = \text{diag}(m_u^2, m_c^2, m_t^2) \\ (\mathbf{D}^D)^2 &= U_L'(\mathbf{M}^D\mathbf{M}^{D\dagger})U_L'^\dagger = \text{diag}(m_d^2, m_s^2, m_b^2) \end{aligned} \quad (14)$$

one can perform the diagonalization to find the CKM mixing matrix, $V_{CKM} = U_L U_L'^\dagger$. The J -value follows from the imaginary part of the commutator determinant from which $\sin \delta$ can be determined.

The following search procedure is then employed.

- (1) Pick a top quark mass and vary the free mass matrix parameters. All $|(V_{CKM})_{ij}|$ are required to fit the experimental values to within one standard deviation accuracy.
- (2) Find J from the commutator determinant and $\sin \delta$ from J and the $|(V_{CKM})_{ij}|$. The first-second quadrant ambiguity for δ is taken into account.
- (3) Impose the additional constraints on the following parameters:

$$\begin{aligned} 0.07 &\leq |V_{ub}/V_{cb}| \leq 0.15 \\ 1.3 &\leq |V_{td}^* V_{tb}|^2 S \simeq (1.8 \pm 0.3) \frac{(0.140)^2}{B_B F_B^2} \leq 2.3 \\ 0.55 &\leq B_K \leq 0.90 \end{aligned} \quad (15)$$

- (4) Repeat the procedure for different m_t .

Two peaks occur in the top quark mass probability distributions, especially for $\cos \delta > 0$, with $F_B \sqrt{B_B} = 140 \pm 25$ MeV as shown in Fig. 1. In Fig. 2 we show the combined distribution for δ in either quadrant with the two peaks corresponding to

$$m_t = \begin{cases} 135 \pm 25 \text{ GeV} \\ 300 \pm 100 \text{ GeV} \end{cases} \quad (16)$$

with the lower mass strongly preferred. For this preferred solution, the corresponding value of ϵ'/ϵ is

$$\epsilon'/\epsilon = (0.8_{-0.2}^{+0.4}) \times 10^{-3} \quad (17)$$

in better agreement with the value of the E731 Fermilab experiment. If J is limited to the range $0.25 < J < 0.35$, the secondary peak at the very high top quark mass is eliminated, but it is probably premature to consider such a restricted range. If, on the other hand, the decay constant is increased to $F_B\sqrt{B_B} = 200 \pm 25$ MeV, the primary peak broadens and becomes more skewed as the secondary peak disappears as also shown in Fig. 2. We believe the former choice is more realistic, however.

RARE B DECAY: $B \rightarrow \gamma + X_{S=1}$

In time, the rare K and B decay processes will also be able to place limits on the top quark mass. One mode of special interest is the inclusive electromagnetic decay of the B meson involving a strangeness +1 final state. Present upper limits on the partial decay rates bound the inclusive process by

$$BR(B \rightarrow \gamma X_s) \lesssim \text{few} \times 10^{-3} \quad (18)$$

The amplitude for $b \rightarrow s + \gamma$ found from the electromagnetic penguin diagrams with internal charm and top quark lines is expressed by

$$\begin{aligned} A(b \rightarrow s\gamma) = \sqrt{2} G_F \frac{e}{16\pi^2} m_b [& V_{ts}^* V_{tb} F(x_t) \bar{s}_L \sigma^{\mu\nu} b_R F_{\mu\nu} \\ & + V_{cs}^* V_{cb} F(x_c) \bar{c}_L \gamma^\mu b_L \bar{s}_L \gamma_\mu c_L] \end{aligned} \quad (19)$$

in terms of the magnetic moment and 4-quark operators, where x_t is given as before and $x_c = m_c^2/M_W^2$.

Ali and Greub [23] have recently calculated the QCD corrections to the penguin graphs, including all gluon bremsstrahlung insertions on the fermion lines, with the W - and quark-exchanges integrated out. They find that $BR(b \rightarrow sg\gamma)$ is a slowly-rising function of m_t in the range $3 \rightarrow 4.5 \times 10^{-4}$ for $100 < m_t < 260$ GeV. The hard part of the photon spectrum, $E_\gamma > 1.6$ GeV is particularly sensitive to m_t . The full

inclusive photon spectrum for $B \rightarrow \gamma + X_{S=1}$ is obtained by including the virtual gluon exchange graph to cancel the IR divergence at $E_g = 0$. It should thus be possible to check these SM predictions at CLEO in 1 - 2 years. A two-Higgs doublet model would be expected to give an even larger branching ratio, for example.

CONCLUSIONS

(1) All the analyses for the SM flavor-changing processes described are in basic agreement. For central values of $B_B F_B^2$ one can not rule out $m_t \gg 200$ GeV on the basis of the flavor-changing data alone.

(2) However, the most probable top quark mass is found to lie in the range 120 - 150 GeV in good agreement with that deduced from the neutral-current data. [24]

(3) The quark mass matrix approach described with a hierarchical structure, though not precisely of the form suggested originally by Fritzsch, leads to similar results.

(4) The rare B decay, $B \rightarrow \gamma + X_{S=1}$ should be observable at CLEO after one-order-of-magnitude improvement in the decay rate, with this process also sensitive to the top quark mass.

ACKNOWLEDGEMENTS

The author acknowledges the kind hospitality of the Fermilab Theoretical Physics Department during the period this contribution was prepared and written. This research was supported in part by Grant No. PHY-8907806 from the National Science Foundation. Fermilab is operated by Universities Research Association, Inc. under contract with the United States Department of Energy.

References

- [1] N. Cabibbo, *Phys. Rev. Lett.* **10** (1963) 531; M. Kobayashi and T. Maskawa, *Prog. Theor. Phys.* **49** (1973) 652.
- [2] Particle Data Group, *Phys. Lett.* **B239** (1990); L. Wolfenstein, *Phys. Rev. Lett.* **51** (1984) 1945.
- [3] C. Jarlskog, *Phys. Rev. Lett.* **55** (1985) 1039 and *Zeit. Phys.* **C29** (1985) 491.
- [4] K. R. Schubert, in *Proceedings of the 1987 EPS Conference*, Uppsala, 1987.
- [5] M. V. Danilov, in *Proceedings of the XIV International Symposium on Lepton and Photon Interactions*, Stanford, 1989; D. L. Kreinick, *ibid.*
- [6] J. S. Hagelin, *Phys. Rev.* **D20** (1979) 2893.
- [7] T. Inami and C. S. Lim, *Progr. Theor. Phys.* **65** (1981) 297.
- [8] A. J. Buras, M. Jamin and P. H. Weisz, Max Planck preprint MPI-PAE/PTh 20/90.
- [9] F. J. Gilman and M. B. Wise, *Phys. Rev.* **D27** (1983) 1128.
- [10] W. A. Bardeen, A. J. Buras and J.-M. Gérard, *Phys. Lett.* **B211** (1988) 343.
- [11] T. T. Wu and C. N. Yang, *Phys. Rev. Lett.* **13** (1964) 380.
- [12] NA31 Collab., H. Burkhardt et al., *Phys. Lett.* **B206** (1988) 169; E731 Collab., J. Patterson et al., *Phys. Rev. Lett.* **64** (1990) 1491.
- [13] A. I. Vainshtein, V. I. Zakharov and M. A. Shifman, *JETP* **45** (1977) 670.
- [14] G. Buchalla, A. J. Buras and M. K. Harlander, *Nucl. Phys.* **B337** (1990) 313.

- [15] E. A. Paschos, T. Schneider and Y. L. Wu, Fermilab preprint FERMILAB-CONF-90/48-T.
- [16] C. Dib, I. Dunietz, F. J. Gilman and Y. Nir, *Phys. Rev.* **D41** (1990) 1522.
- [17] J. F. Gunion and B. Gradkowski, *Phys. Lett.* **B243** (1990) 301.
- [18] Ref. [14] and D. Cocolicchio and J.-R. Cudell, CERN preprint CERN-TH 5729/90.
- [19] C. S. Kim, J. L. Rosner and C.-P. Yuan, *Phys. Rev.* **D42** (1990) 96.
- [20] J. Maalampi and M. Roos, *Particle World* **1** (1990) 148.
- [21] C. H. Albright, *Phys. Lett. B*, to be published; *Three-Family Top Quark Mass Spectrum*, Fermilab preprint FERMILAB-CONF-90/104-T.
- [22] H. Fritzsch, *Phys. Lett.* **B70** (1977) 436; **B73** (1978) 317; **B186** (1986) 423.
- [23] A. Ali and C. Greub, DESY preprint DESY 90-102 and references contained therein.
- [24] J. Ellis and G. L. Fogli, *B* **232** (1989) 139 and CERN preprint CERN TH-5817-90; P. Langacker, *Phys. Rev. Lett.* **63** (1989) 1920.

Figure Captions

Figure 1: Top quark mass probability distribution in the mass matrix approach with $F_B\sqrt{B_B} = 140 \pm 25$ MeV, where the solid (dashed) histogram refers to δ in the first (second) quadrant.

Figure 2: Top quark mass distributions for δ in either quadrant and $F_B\sqrt{B_B} = 140 \pm 25$ MeV for the solid histogram and $F_B\sqrt{B_B} = 200 \pm 25$ MeV for the dashed histogram.

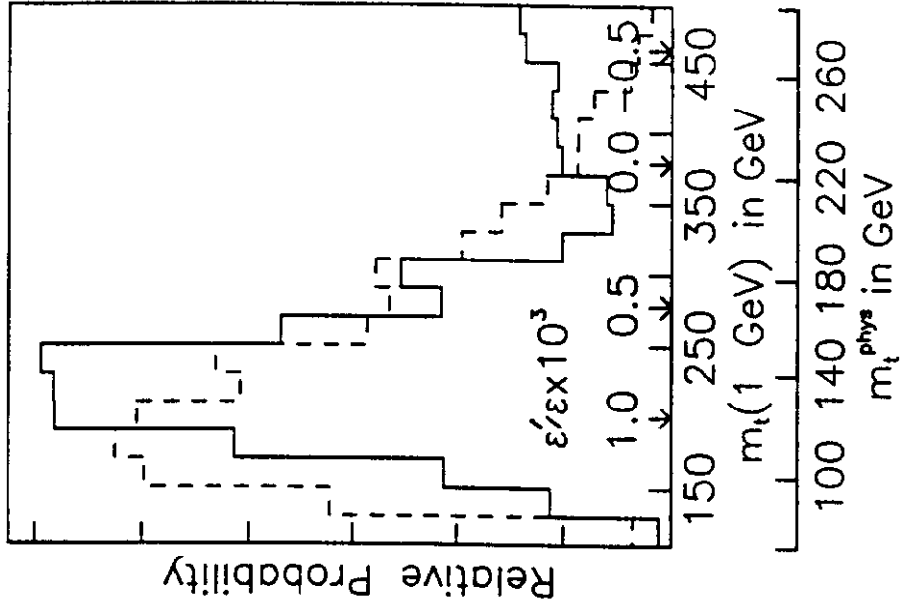


Fig. 2

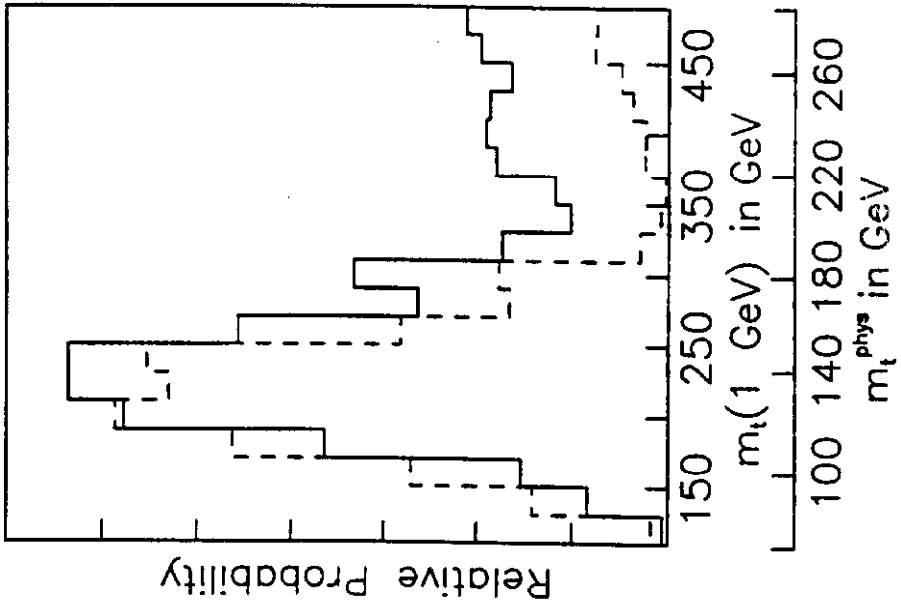


Fig. 1